

[doi:10.2109/jcersj2.123.1084](https://doi.org/10.2109/jcersj2.123.1084)

Effect of the template ion exchange behaviors of chromium into FSM-16 on the oxidative dehydrogenation of isobutane

Takuya EHIRO, Ai ITAGAKI, Masashi KURASHINA,* Masahiro KATOH, Keizo NAKAGAWA,**,***
Yuuki KATOU,**** Wataru NINOMIYA**** and Shigeru SUGIYAMA**,*****

Department of Chemical Science and Technology, Tokushima University, Minamijosanjima, Tokushima 770-8506, Japan

***Department of Life System, Institute of Technology and Science, Tokushima University,
Minamijosanjima, Tokushima 770-8506, Japan**

****Department of Advanced Materials, Institute of Technology and Science, Tokushima University,
Minamijosanjima, Tokushima 770-8506, Japan**

*****Department of Resource Circulation Engineering, Center for Frontier Research of Engineering, Tokushima University,
Minamijosanjima, Tokushima 770-8506, Japan**

******Otake Research Laboratories, Mitsubishi Rayon Co. Ltd., 20-1 Miyuki-cho, Otake, Hiroshima 739-0693, Japan**

Effect of the template ion exchange behaviors of chromium into FSM-16 on the oxidative dehydrogenation of isobutane

Takuya EHIRO, Ai ITAGAKI, Masashi KURASHINA,* Masahiro KATOH,** Keizo NAKAGAWA,**,*** Yuuki KATOU,**** Wataru NINOMIYA**** and Shigeru SUGIYAMA**,**,***,†

Department of Chemical Science and Technology, Tokushima University, Minamijosanjima, Tokushima 770-8506, Japan

*Department of Life System, Institute of Technology and Science, Tokushima University,

Minamijosanjima, Tokushima 770-8506, Japan

**Department of Advanced Materials, Institute of Technology and Science, Tokushima University,

Minamijosanjima, Tokushima 770-8506, Japan

***Department of Resource Circulation Engineering, Center for Frontier Research of Engineering, Tokushima University,

Minamijosanjima, Tokushima 770-8506, Japan

****Otake Research Laboratories, Mitsubishi Rayon Co. Ltd., 20-1 Miyuki-cho, Otake, Hiroshima 739-0693, Japan

The template ion exchange of chromium cations into FSM-16 (#16 Folded Sheets Mesoporous Materials) for 247 h resulted in a 2.89 wt % incorporation of those cations into the FSM-16, although only a 0.3 wt % incorporation had previously been reported. The XRD pattern of the resultant solid (Cr-FSM-16) showed that the hexagonal structure characteristic of FSM-16 remained after the 2.89 wt % incorporation of chromium cations. XPS could be used to detect the Cr³⁺ and Cr⁶⁺ species on the surface of Cr-FSM-16. A pre-edge peak that was due to a tetrahedrally coordinated Cr⁶⁺ species was confirmed in the XANES spectrum of the Cr-FSM-16, which showed that the coordination state around some Cr species was similar to that around the Si species in FSM-16. With the increase in the amount of chromium cations in FSM-16, its catalytic activity and stability during the oxidative dehydrogenation of isobutane were evidently improved.

©2015 The Ceramic Society of Japan. All rights reserved.

Key-words : Template ion exchange, FSM-16, Chromium, Oxidative dehydrogenation, Isobutane

[Received August 19, 2015; Accepted September 27, 2015]

1. Introduction

In our laboratory, a template ion exchange (TIE) procedure using mesoporous silica has been developed to prepare an active catalyst. This procedure was first employed for MCM-41 (#41 Mobil Composition of Matter).¹⁾ For example, Si-sources such as colloidal silica and template surfactants such as [C₁₂H₂₅N-(CH₃)₃]⁺Br⁻ can be used to obtain “as-synthesized MCM-41” before calcination, in which the surfactant remains.²⁾ In the TIE procedure, Mn²⁺ was exchanged with template cation in as-synthesized MCM-41.²⁾ During the ion exchange, the amount of template cation released was correlated with the amount of incorporated Mn²⁺, as a stoichiometric exchange.³⁾ This is why the name “template” is used in reference to the TIE procedure. Based on this study, various metal cations could be incorporated into MCM-41 to be used as active catalysts for some reactions.³⁾ More recently, MCM-41 incorporated with Ni²⁺ (Ni-MCM-41) has been prepared using the TIE procedure, which resulted in great catalytic activity for the conversion of ethylene to propylene.⁴⁾ In the case of Ni-MCM-41, the Ni²⁺ in Ni-MCM-41 has a layered nickel silicate-like structure similar to NiO₆ layer that is sandwiched by one or two silica layers.⁴⁾ In contrast, when Ni²⁺ is substituted for the Si⁴⁺ in a MCM-41 framework, it results in a tetragonal coordination of the structure, such as with NiO₄.⁵⁾ In our previous studies,^{6),7)} the incorporation of 0.3 wt % chromium cations into another mesoporous silica, FSM-16 (#16

Folded Sheets Mesoporous Materials), via the TIE procedure showed great activity for the oxidative dehydrogenation of isobutane to isobutene. FSM-16, which was first reported by Inagaki et al. in 1993,⁸⁾ featured characteristics such as a hexagonal structure and rather strong acidic properties that are typical of mesoporous silica, MCM-41. It is generally accepted that FSM-16 is formed via layered intermediates composed of fragmented silicate sheets and alkyltrimethylammonium cations.⁹⁾ Hence, the formation mechanism is different from that of MCM-41, resulting in unique catalytic activities on silicious or metal-containing FSM-16.⁹⁾ Also, it is generally accepted that the preparation of MCM-41 requires hydrothermal conditions that result in the formation of thermally unstable mesoporous silica. By contrast, hydrothermal conditions are unnecessary for the preparation of FSM-16, which is a mesoporous silica that is thermally stable.⁸⁾ Furthermore, Ni²⁺ was incorporated into FSM-16 via the TIE procedure, and the resultant solid showed great catalytic activity in a conversion of ethanol to propylene.¹⁰⁾ In the TIE procedure, mesoporous silica such as MCM-41 or FSM-16 was not directly used, while a precursor of mesoporous silica (as-synthesized MCM-41 or FSM-16), a dried solid mixture consisting of a silica-source and a template surfactant, was used for the ion exchange with various cations. This demonstrated that the TIE procedure for the incorporation of various cations into mesoporous silica is a unique preparation procedure for an active catalyst. However, the TIE behavior between the precursors of mesoporous silica, particularly the precursor for FSM-16 (as-synthesized FSM-16) and cations, remains unclear. Furthermore, little information is available concerning the structure of

† Corresponding author: S. Sugiyama; E-mail: sugiyama@tokushima-u.ac.jp

FSM-16 with incorporated cations, as prepared using the TIE procedure.

In the present study, the TIE behavior between as-synthesized FSM-16 and Cr cations was examined. Then, the structure of the resultant solid (Cr-FSM-16) was characterized using XRD (X-ray diffraction), XPS (X-ray photoelectron spectroscopy), XAFS (X-ray absorption fine structure), TEM (transmission electron microscope) and N_2 adsorption–desorption isotherms, while the acidic properties were analyzed using NH_3 -TPD (temperature-programmed desorption of NH_3). Furthermore, the catalytic activity during the oxidative dehydrogenation of isobutane on Cr-FSM-16 was also examined.

2. Experimental

2.1 Template ion exchange between as-synthesized FSM-16 and chromium cations

A hydrated sodium silicate powder (Kishida Chemical Co. Ltd., Osaka, Japan; a molar ratio of $SiO_2/Na_2O = 2.00$) as a silicate source and cetyl trimethyl ammonium bromide (Wako Pure Chemical Industries, Ltd., Osaka, Japan; (CTA)Br) as a template reagent were used for the preparation for FSM-16, according to a procedure established by Inagaki et al.^{8),11)} After the calcination of the hydrated sodium silicate powder at 973 K for 6 h, the resultant solid was ground, added to distilled water, and then stirred for 3 h at room temperature. During the stirring, the calcined solid converted to kanemite ($NaHSi_2O_5 \cdot 3H_2O$). Kanemite was separated using a centrifuge and was added to an aqueous solution consisting of (CTA)Br. The solution was refluxed at 343 K for 3 h and then cooled to room temperature. The solution pH was adjusted to 8.5 using 2 M HCl and then stirred at 343 K for 18 h. The resultant solid sample was washed, filtered and dried at 333 K to obtain a white solid sample, which was denoted as “as-synthesized FSM-16”. Finally, FSM-16 was obtained by calcination of as-synthesized FSM-16 at 823 K for 8 h.

In order to examine the TIE behaviors, the as-synthesized FSM-16 (5 g) was dispersed in 50 mL of distilled water. After 10 mL of 0.50 M $Cr(NO_3)_3 \cdot 9H_2O$ (Sigma-Aldrich Japan) was added to the dispersed solution with vigorous stirring for 1 h, the temperature was adjusted to 353 K, according to the original procedure.^{1)–4)} This segment was referred to as the start time of TIE (0 h TIE). The TIE behaviors were monitored using ICP-AES (SPS3520UV, SII Nanotechnology). In the present study, the concentration of Cr cations incorporated into as-synthesized FSM-16 and that of Si cations released from as-synthesized FSM-16 were monitored. The resultant solid obtained after x h TIE was described as “ x h Cr-FSM-16”.

2.2 Characterization

The solid samples, FSM-16 and Cr-FSM-16, were characterized using XRD (RINT 2500X, Rigaku Co.), N_2 adsorption–desorption measurement (BELSORP-18SP, Bel Japan Inc.), and TEM (JEM-2100F, JEOL Ltd.). The powder XRD patterns of the solid samples were obtained using monochromatized $CuK\alpha$ radiation (40 kV, 40 mA). Before the N_2 adsorption–desorption measurement at 77 K, the solid sample was pretreated at 473 K for 10 h in a vacuum. The TEM images of the solid samples were obtained at an accelerating voltage of 200 kV. In order to detect the fine structure changes around the Cr species in Cr-FSM-16, XAFS measurement was performed with synchrotron radiation at the BL9A station of the Photon Factory in the High Energy Accelerator Research Organization (Tsukuba, Japan). A storage ring current was 450 mA (2.5 GeV). The X-rays were mono-

chromatized with Si(111). The redox properties of the Cr species on the surface of Cr-FSM-16 were evaluated using XPS (PHI-5000VersaProbe II, ULVAC-PHI Inc.). The XPS spectra were calibrated based on the C 1s peak at 285.0 eV. The acidic properties of FSM-16 and Cr-FSM-16 were estimated using NH_3 -TPD (BELCAT-A-SP, Bel Japan Inc.). In NH_3 -TPD, a solid sample (50 mg) was heated to 773 K at a rate of 10 K/min under a He flow [50.0 sccm (standard cubic centimeter per min)], and was then held at this temperature for 1 h under the He flow. Then the sample was cooled to 373 K under the He flow, and held at this temperature for 10 min. The solid sample was then treated with 5% NH_3/He (50.0 sccm) for 30 min. After the treatment, He was replenished (50.0 sccm) and the solid sample was kept in the He flow for 15 min. Then, the solid sample was heated from 373 to 773 K at a rate of 10 K/min under He flow (30.0 sccm). The desorbed NH_3 from the solid sample during the final process was analyzed using a quadrupole mass spectrometer (OmniStar-s, Pfeiffer Vacuum GmbH). A fragment peak at $m/e = 16$ was used to monitor the NH_3 .

2.3 Catalytic activity test

The oxidative dehydrogenation of isobutane on FSM-16 and Cr-FSM-16 were carried out in a fixed-bed continuous flow reactor at atmospheric pressure. Each catalyst (0.25 g) was molded by wet-treatment to 0.85–1.70 mm to maintain the hexagonal structure of FSM-16.¹²⁾ They were fixed with quartz wool and pretreated with 12.5 mL/min of O_2 gas flow at 723 K. After the pretreatment, catalytic activity tests were started by flowing 15 mL/min of helium, isobutane and oxygen to the reactor. Their partial pressures were adjusted to $P(i-C_4H_{10}) = 14.4$ kPa, and $P(O_2) = 12.3$ kPa diluted with He. Under these conditions, no homogeneous gas phase reaction was observed. The reaction was monitored using an online gas chromatograph (Shimadzu GC-8APT) equipped with a TCD. A Molecular Sieve 5A (MS 5A, 0.2 m \times Φ 3 mm) for O_2 , CH_4 and CO and a Hayesep R (2.0 m \times Φ 3 mm) for CO_2 , C_2 , C_3 , and C_4 products were used as the columns. The carbon balance between the reactant and the products was within $\pm 5\%$. The product selectivity and isobutane conversion were calculated on a carbon basis.

3. Results and discussion

3.1 TIE behaviors of chromium ions into as-synthesized FSM-16

Figure 1 presents the TIE behaviors of Cr cations toward as-synthesized FSM-16 at 353 K. In Fig. 1, the start time of the TIE was 0 h, and the TIE solution temperature was adjusted to 353 K. The TIE solution had already been stirred at room temperature for 1 h before the adjustment of the solution temperature to 353 K, according to the original procedure.^{1)–4)} Therefore, a certain amount of Si cations (0.83 mmol/L) was released to the aqueous solution that consisted of Cr cations until the start time, while a negligible amount of Cr cations (0.04 mmol/L) was incorporated into as-synthesized FSM-16. This indicates that the dissolution of as-synthesized FSM-16 proceeded extensively by the start time while the ion exchange hardly proceeded. It is noteworthy that the releasing behavior of Si cations was similar to the incorporated behavior of Cr cations after the start time. The difference between the amounts of Si cations released at 0 and 247 h (0.83 and 2.90 mmol/L, respectively) was 2.07 mmol/L, while that of Cr cations incorporated at 0 and 247 h (0.04 and 1.50 mmol/L, respectively) was 1.46 mmol/L. Therefore, the molar ratio of the Si that was released compared with the incorporated Cr was 1.42. As described below, Cr^{3+} and Cr^{6+}

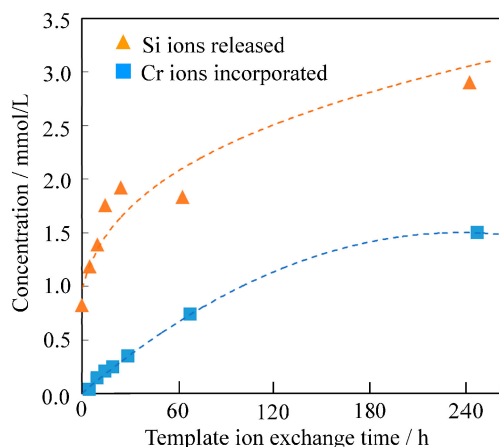


Fig. 1. Relationships between the amount of Si ions released from as-synthesized FSM-16 and that of Cr ions incorporated into as-synthesized FSM-16 during the TIE at 353 K.

Table 1. Cr loading, surface area, pore volume, pore size and ratio of acid amount of each Cr-FSM-16 against FSM-16

	Cr loading ^a /wt %	Surface area ^b /m ² g ⁻¹	Pore volume ^b /cm ³ g ⁻¹	Pore size ^b /nm	Acidic ratio ^c /—
FSM-16	0	871	1.15	5.27	1.00
0 h Cr-FSM-16	0.08	881	1.20	5.47	1.91
1 h Cr-FSM-16	0.28	776	1.11	5.72	2.36
5 h Cr-FSM-16	0.41	916	1.24	5.41	2.27
10 h Cr-FSM-16	0.49	930	1.19	5.14	2.18
20 h Cr-FSM-16	0.68	851	1.17	5.48	2.97
60 h Cr-FSM-16	1.44	854	1.10	5.17	3.74
247 h Cr-FSM-16	2.89	754	1.14	6.06	11.45

a ICP-AES. b N₂ adsorption–desorption measurement. c Ratio of acid amount of each Cr-FSM-16 against that of FSM-16 estimated using NH₃-TPD.

contributed to the present system. If the direct and stoichiometric ion exchange between Si⁴⁺ in as-synthesized FSM-16 and Cr³⁺ proceeds during the TIE, the molar ratio should have been 1.33. However, for the direct ion exchange between Si⁴⁺ in as-synthesized FSM-16 and Cr⁶⁺, the molar ratio should have been 0.67. Although it is evident that the molar ratio estimated in the present study may have been overestimated due to the dissolution of Si cations from as-synthesized FSM-16, it is noteworthy that the estimated molar ratio is the same order postulated via the direct and stoichiometric ion exchange between Si⁴⁺ in as-synthesized FSM-16 and chromium cations. The loadings of Cr species in each Cr-FSM-16 estimated from the data in Fig. 1 are listed in Table 1 with other correlated information. In our previous studies,^{6,7} Cr cations could be incorporated into FSM-16 at only 0.3 wt %, while the loading was improved up to 2.89 wt % after 247 h of TIE.

3.2 Characterization of FSM-16 and Cr-FSM-16

Figure 2 shows the XRD patterns of FSM-16, 0 h Cr-FSM-16 and 247 h Cr-FSM-16. Each of the peaks obtained at the lower diffraction angles [Fig. 2(a)] matched the three diffraction peaks due to the hexagonal structure of FSM-16; those peaks were assigned to (100), (110) and (200) planes from the lowest diffraction angles.⁸ Three peaks at approximately 22 degrees could be ascribed to tridymite (JCPDS 421401) as reported by Ikeue

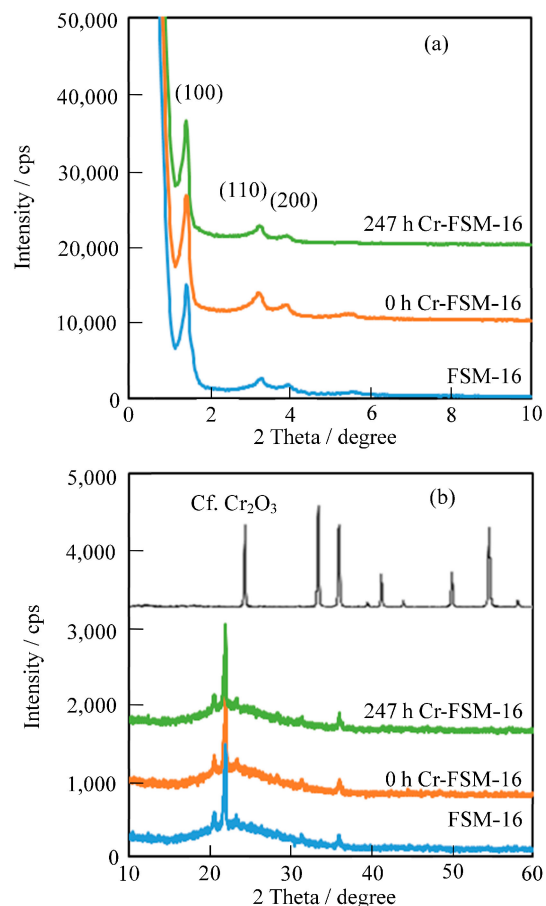


Fig. 2. XRD patterns of FSM-16, 0 h Cr-FSM-16, and 247 h Cr-FSM-16 detected from (a) lower and (b) higher diffraction angles.

et al.¹³) Kanemite, which is finally converted to FSM-16, is produced through δ -Na₂Si₂O₅.⁹) To synthesize pure kanemite, Na/Si molar ratio of the precursor should be kept at 1.0 during the synthesis while the control of the calcination temperature of the sodium silicate powder is important for the formation of pure δ -Na₂Si₂O₅. In the present study, those factors may contribute to degradation of the purity of the produced δ -Na₂Si₂O₅ followed by the formation of tridymite. Although an excess amount of Cr species was introduced into FSM-16 (247 h Cr-FSM-16), there were no peaks at the lower diffraction angles due to Cr species, indicating the maintenance of the hexagonal structure. If the formation of Cr₂O₃ proceeds during the TIE, some peaks should be detected at the higher diffraction angles (JCPDS 381479). However, no peaks due to Cr₂O₃ were evident [Fig. 2(b)], indicating that, in contrast with those observed using a typical impregnation procedure, chromium oxides were not supported on FSM-16. It is noteworthy that the intensity of a peak due to (100) planes was decreased with an increase in the amount of Cr species incorporated into FSM-16. The ionic radius of Si⁴⁺ was shorter than those of Cr³⁺ or Cr⁶⁺ (0.069 and 0.052 nm, respectively). Therefore, if the ion exchange of Si⁴⁺ in FSM-16 with Cr³⁺ or Cr⁶⁺ proceeded during the TIE, the decrease in the intensity was reasonable due to a slight distortion in the ordered structure.

The maintenance of the hexagonal structure of Cr-FSM-16 was further supported by TEM and N₂ adsorption–desorption measurements. As shown in Fig. 3 for FSM-16, 0 h Cr-FSM-16, and 247 h Cr-FSM-16, a hexagonal structure was detected in the TEM

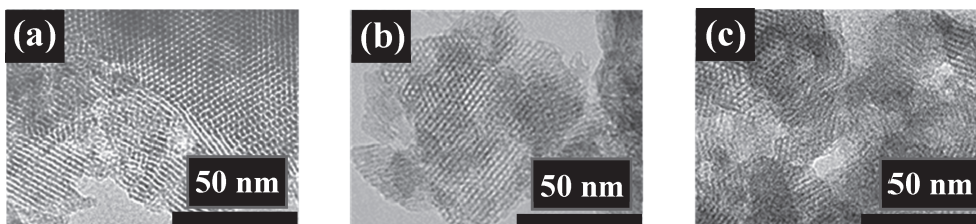
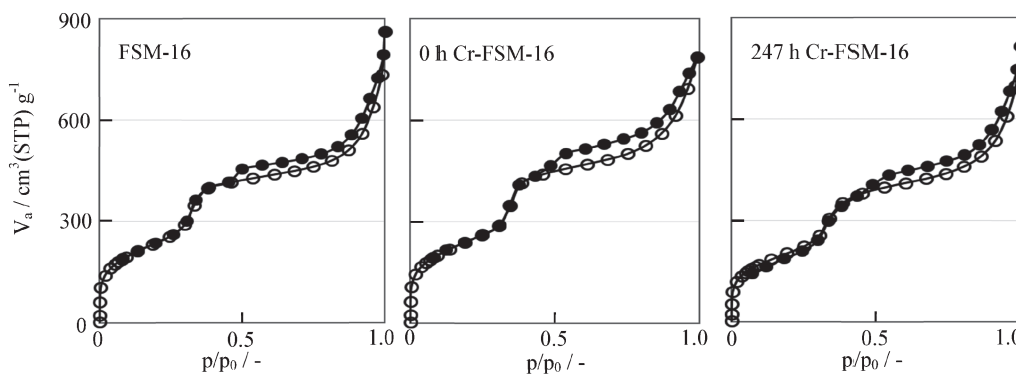


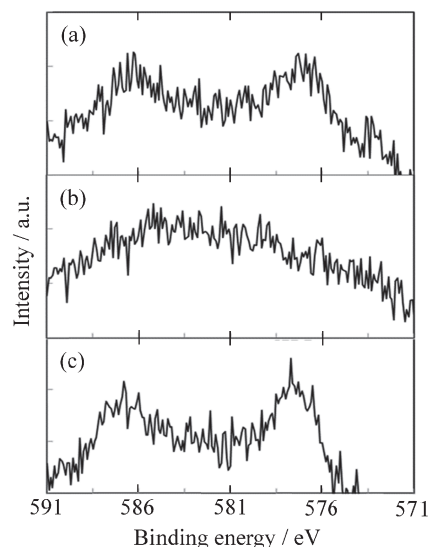
Fig. 3. TEM images of FSM-16, 0h Cr-FSM-16, and 247h Cr-FSM-16.

Fig. 4. N₂ adsorption-desorption isotherms for FSM-16, 0h Cr-FSM-16, and 247h Cr-FSM-16.

of FSM-16 and in all the Cr-FSM-16 prepared in the present study. Furthermore, typical type IV curves with hysteresis loops that indicate the presence of mesopores, were also detected via N₂ adsorption-desorption isotherms from all the samples (Fig. 4 for FSM-16, 0h Cr-FSM-16 and 247h Cr-FSM-16 as examples). Values for the specific surface areas, pore volumes and pore sizes that were estimated from those adsorption-desorption curves are shown in Table 1. Since these data did not correlate to Cr-loading and were almost identical, those data support that these samples retained the hexagonal structure that is characteristic to the parent FSM-16, while the surface area of FSM-16 prepared in the present study (871 m²/g) was smaller than those previously reported.

For example, the greater surface areas such as 815–1078 m²/g supplied by Toyota Central R & D labs, Inc. (Lot no. NG78-550),¹⁴ as well as 1070 and 1100 m²/g prepared by Inagaki et al.⁸) were reported. The smaller surface area of FSM-16 prepared in the present study would indicate that it contains tridymite as impurities. If Cr species are introduced into FSM-16 through one mode, those data should correlate to Cr-loading. Therefore the introduction of Cr species into FSM-16 may proceed through some modes together with the TIE.

Although it was evident that the incorporation of a Cr species into FSM-16 via TIE did not influence the hexagonal structure that is characteristic to mesoporous silica, no information on Cr-species was obtained from XRD, TEM or N₂ adsorption-desorption measurements. Therefore, XPS and XAFS analyses were employed for the characterization of Cr species. The XPS spectrum of fresh 60h Cr-FMS-16 is described in Fig. 5(a). Two broad peaks due to Cr 2p_{3/2} and Cr 2p_{1/2} were detected at 576.9 and 586.1 eV (interval = ca. 9 eV), respectively. Similar XPS results were reported from SBA-15 doped with Cr species.¹⁵ Furthermore, Cr 2p_{3/2} and 2p_{1/2} were detected at 576.5 and 585.5 eV (interval = 9 eV) for Cr³⁺ and at 579.0 and 587.5 eV (interval = ca. 9 eV) for Cr⁶⁺, respectively.¹⁵ Comparing the XPS spectrum of 60h Cr-FSM-16 with that of SBA-15 doped

Fig. 5. XPS spectra obtained from the region due to Cr 2p_{1/2} and Cr 2p_{3/2} of (a) fresh, (b) after the reaction, and (c) after the oxygen treatment of 60h Cr-FSM-16 previously used in obtaining the result shown Fig. 5(b).

with Cr species, it was evident that there were fewer Cr⁶⁺ species on 60h Cr-FSM-16 along with Cr³⁺ species. Furthermore, the Cr K-edge XANES spectrum of 247h Cr-FSM-16 revealed valuable information on the Cr species. As shown in Fig. 6, a pre-edge peak at ca. 5990 eV was detected along with a typical absorption spectrum. The pre-edge obtained from Cr-containing mesoporous silica represented tetrahedrally coordinated Cr⁶⁺ species.^{16,17} Therefore the Cr K-edge XANES indicates the presence of Cr⁶⁺ together with Cr³⁺ species. It is noteworthy that the coordination state around Cr species in 60h Cr-FSM-16 was similar to that around the Si in FSM-16. This may indicate that some Si⁴⁺

in FSM-16 was directly exchanged with Cr species during the TIE.

3.3 Catalytic activity for the oxidative dehydrogenation of isobutane on Cr-FSM-16

Figure 7 represents the results obtained from the oxidative dehydrogenation of isobutane on the Cr-FSM-16 catalysts prepared in the present study.

In previous reports, the parent FSM-16 showed low catalytic activity for the present reaction such as a 15.1% conversion of isobutane, a selectivity to isobutene at 8.8%, and a 1.3% yield of isobutene under the same reaction conditions.⁷⁾ Upon the addition of the Cr species into FSM-16 using a TIE time of between 0 and 1 h (0 and 1 h Cr-FSM-16), both the conversion and the selectivity were improved, resulting in an enhancement in the yield of isobutene of as much as 2%, as shown in our previous study.⁷⁾ Further extension of the TIE time to 10 h resulted in an evident improvement (up to 24%) in the selectivity to isobutene from the initial time-on-stream of 3.25 h for the yield of isobutene (5 and 10 h Cr-FSM-16). Unfortunately, an evident deactivation was detected on both catalysts at 4.5 h on-stream and longer. However, a further extension of the TIE time of longer than 20 h resulted in greater and more stable activities at the 20, 60 h and finally at 247 h Cr-FSM-16 to achieve a 6.6% yield of isobutene. These results reveal that increases in the loading of Cr species into FSM-16 with increases in the TIE time (Table 1) resulted in an evident improvement in both the catalytic activity and stability.

In our previous paper,⁷⁾ when 0.3% Cr-FSM-16, Cr-species with weak acidic properties and redox nature contributed to the catalytic activity. Therefore, NH_3 -TPD was used to examine the

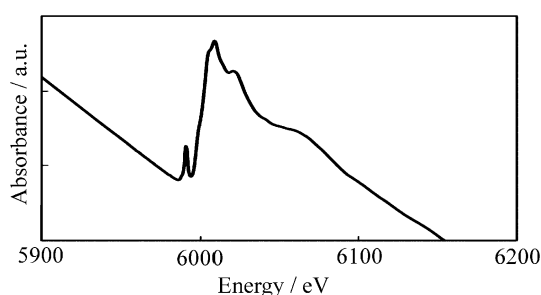


Fig. 6. Cr K-edge XANES spectra of 247 h Cr-FSM-16.

acidic properties of FSM-16 and Cr-FSM-16. As shown in **Fig. 8**, NH_3 -desorption peaks were detected at temperatures between 373 and 673 K as reported in our previous paper.⁷⁾ In Table 1, the acidic ratio for each form of Cr-FSM-16 against that of FSM-16 are described as estimated from the data in Fig. 8, indicating that the acid amount tended to increase with the TIE time and the Cr loading. Therefore, it was again confirmed that Cr species with weak acidic properties contributes to catalytic activity, although when an excess amount of Cr species was introduced into FSM-16, as shown in data for 60 h Cr-FSM-16 and 247 h Cr-FSM-16 (Table 1), it contributed little to the further enhancement of the catalytic activity as shown in the activity of these two catalysts (Fig. 8). It is noteworthy that an increase in the partial pressure of O_2 in the reactant gas to 24.6 kPa resulted in an enhancement in the conversion of isobutane and the selectivity to CO_2 together with a decrease in the selectivity to isobutene, which resulted in a similar yield of isobutene: $P(\text{O}_2) = 12.3$ kPa.

Finally, the redox nature of the Cr species was examined using XPS. Two broad peaks at 576.9 and 586.1 eV were detected from fresh 60 h Cr-FSM-16 due to Cr $2p_{3/2}$ and Cr $2p_{1/2}$ [Fig. 5(a)], but were not observed from that previously used for the catalytic reaction, and a broader peak was detected over a wider range of binding energy [Fig. 5(b)]. This behavior would be reasonable if the Cr species in the catalyst was reduced during the reaction to form various oxidation states of Cr-species. Upon the treatment of the catalyst shown in Fig. 5(b) using gaseous O_2 at 723 K for 2 h, two broad peaks were observed, as shown in Fig. 5(a), and were again regenerated [Fig. 5(c)]. In our previous paper, the redox property was detected using H_2 -TPR since the loading of the Cr-species was as low as 0.3%. In the present study, a similar redox property reported in our previous paper⁷⁾ was directly detected in the XPS for Cr species due to the greater loading of the Cr species (1.44%). Therefore, this again confirmed that a Cr species with a redox nature contributes to catalytic activity.

4. Conclusion

Although it is established that the incorporation of a Cr species into FSM-16 directly contributes to an improvement in catalytic activity during the oxidative dehydrogenation of isobutane, when a small amount of the Cr species was added to FSM-16 (Cr loading = 0.3 wt %), this complicated the process of elucidating of the correlation between structure and catalytic activity. In the present study, however, the results from XRD, XANES, XPS,

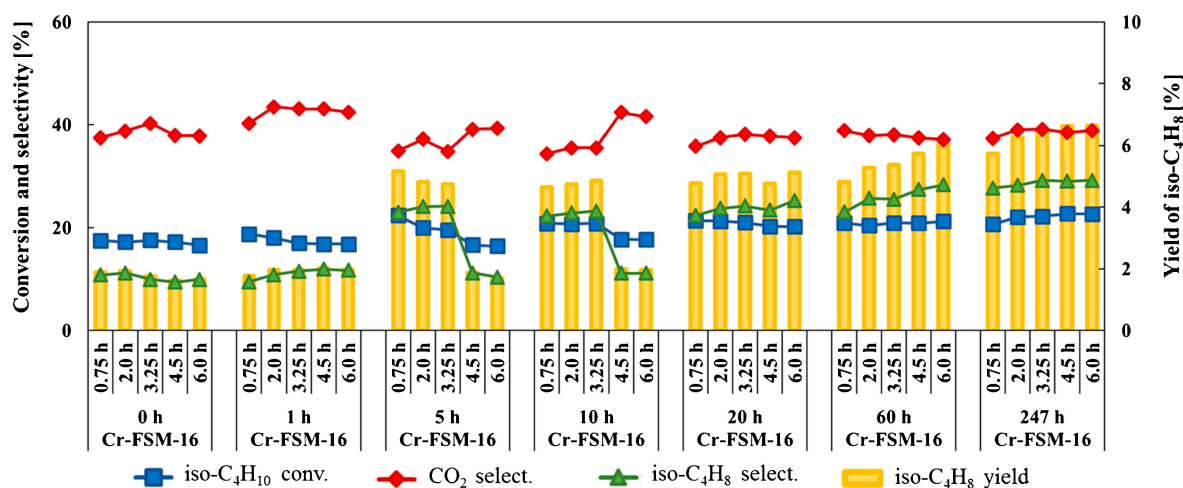


Fig. 7. Catalytic activity of Cr-FSM-16 during the oxidative dehydrogenation of isobutane at 723 K.

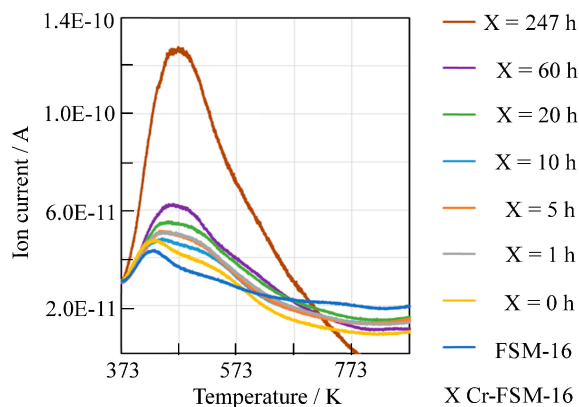


Fig. 8. NH_3 -TPD spectra of FSM-16 and Cr-FSM-16.

and NH_3 -TPD using Cr-FSM-16 obtained via TIE for 247 h (Cr loading = 2.89 wt %) suggested that some of the Si^{4+} in FSM-16 was directly exchanged with Cr^{6+} and that the Cr species with weak acidic properties and a redox nature contributed to the catalytic activity during oxidative dehydrogenation.

References

- 1) C. T. Kresge, M. E. Leonowicz, W. J. Roth, J. C. Vartuli and J. S. Beck, *Nature*, **359**, 710–712 (1992).
- 2) M. Yonemitsu, Y. Tanaka and M. Iwamoto, *Chem. Mater.*, **9**, 2679–2681 (1997).
- 3) M. Iwamoto and Y. Tanaka, *Catal. Surv. Jpn.*, **5**, 25–36 (2001).
- 4) K. Ikeda, Y. Kawamura, T. Yamamoto and M. Iwamoto, *Catal. Commun.*, **9**, 106–110 (2008).
- 5) Y. Yang, S. Lim, G. Du, Y. Chen, D. Ciuparu and G. L. Haller, *J. Phys. Chem. B*, **109**, 13237–13246 (2005).
- 6) S. Sugiyama, Y. Nitta, Y. Furukawa, A. Itagaki, T. Ehiro, K. Nakagawa, M. Katoh, Y. Katou, S. Akihara and W. Ninomiya, *J. Chem. Chem. Eng.*, **7**, 1014–1020 (2013).
- 7) S. Sugiyama, T. Ehiro, Y. Nitta, A. Itagaki, K. Nakagawa, M. Katoh, Y. Katou, S. Akihara, T. Yasukawa and W. Ninomiya, *J. Chem. Eng. Jpn.*, **48**, 133–140 (2015).
- 8) S. Inagaki, Y. Fukushima and K. Kuroda, *J. Chem. Soc. Chem. Commun.*, 680–682 (1993).
- 9) T. Kimura and K. Kuroda, *Adv. Funct. Mater.*, **19**, 511–527 (2009).
- 10) S. Sugiyama, Y. Kato, T. Wada, S. Ogawa, K. Nakagawa and K.-I. Sotowa, *Top. Catal.*, **53**, 550–554 (2010).
- 11) S. Inagaki, A. Koiwai, N. Suzuki, Y. Fukushima and K. Kuroda, *Bull. Chem. Soc. Jpn.*, **69**, 1449–1457 (1996).
- 12) S. Sugiyama, Y. Okada, Y. Kosaka, K. Nakagawa, M. Katoh, Y. Katou, S. Akihara, T. Yasukawa and W. Ninomiya, *J. Chem. Eng. Jpn.*, **46**, 620–624 (2013).
- 13) K. Ikeue, T. Tanaka, N. Miyoshi and M. Machida, *Solid State Sci.*, **10**, 1584–1590 (2008).
- 14) T. Yamamoto, T. Tanaka, T. Funabiki and S. Yoshida, *J. Phys. Chem. B*, **102**, 5830–5839 (1998).
- 15) G. Wang, L. Zhang, J. Deng, H. Dai, H. He and C. T. Au, *Appl. Catal., A*, **355**, 192–201 (2009).
- 16) Y. Wang, Y. Ohishi, T. Shishido, Q. Zhang, W. Yang, Q. Guo, H. Wan and K. Takehira, *J. Catal.*, **220**, 347–357 (2003).
- 17) K. Takehira, Y. Ohishi, T. Shishido, T. Kawabata, K. Takaki, Q. Zhang and Y. Wang, *J. Catal.*, **224**, 404–416 (2004).